Available online at www.sciencedirect.com

SciVerse ScienceDirect

Ceramics International 39 (2013) 1603–1612

CERAMICS INTERNATIONAL

www.elsevier.com/locate/ceramint

Broad band down conversion from ultra violet light to near infrared emission in $YVO_4:Bi^{3+}$, Yb^{3+} as spectral conversion phosphor for c-Si solar cells

U. Rambabu[1], Sang-Do Han*

Korea Institute of Energy Research (KIER), Daejeon 305-343, Republic of Korea

Received 12 July 2012; received in revised form 2 August 2012; accepted 2 August 2012
Available online 8 August 2012

Abstract

Vanadate based down conversion phosphors have been synthesized by a novel co-precipitation technique. The effect of pH on crystal structure, particle size, morphology and luminescence properties were investigated by XRD, SEM-EDAX, FT-IR and PL measurements. As different from other reports (blue, green emission) the produced phosphors have shown greenish–yellow emission, owing to their fine particle size. A broad band excitation (280–370 nm), ascribed to $^1S_0 \rightarrow {}^3P_1$ and an intense greenish–yellow band emission (410–700 nm) attributed to $^3P_1 \rightarrow {}^1S_0$ transition of Bi^{3+} were observed. A strong greenish–yellow emission was measured with 3 mol. % of Bi^{3+} ions, as an optimum dopant concentration. The characteristic NIR emission of Yb^{3+}, owing to $^2F_{5/2} \rightarrow {}^2F_{7/2}$ was recorded at 1039 nm, as a result of efficient energy transfer from Bi^{3+} to Yb^{3+}, ions. The phosphors with chemical composition as $Y_{0.96}VO_4$: $Bi^{3+}_{0.03}$, $Yb^{3+}_{0.01}$ and $Y_{0.87}VO_4$: $Bi^{3+}_{0.03}$,$Yb^{3+}_{0.1}$ are suggested to be the novel candidates for the efficient down conversion of broad band ultra violet (UV) light into visible/near infrared (NIR) emission, as DC layers on c-Si solar cells for better harvesting the solar spectrum via spectral matching phenomena.

Keywords: A. Powder: Chemical preparation; C. Optical properties; C. Color

1. Introduction

Energy problem would be working on over the next quarter of a century as one of the most challenging scientific questions [1]. In order to solve the problem of energy crisis, it is necessary to explore the promising application of green and sustainable energy. As a result, solar energy has been received much attention in recent years. One of the major limits for the efficiency improvement of solar cells is considered to be the mismatch between the incident solar photon spectrum and the band gap of silicon. To reduce the energy losses, including lattice thermalization and sub-band gap transmission loss, spectral modification through (i) down-shifting (DS), (ii) down-conversion (DC) as well as (iii) up-conversion (UP) of photons have been regarded as an effective routes. The second option is to split one higher energy photon to obtain two photons with a lower energy. Each of these photons can subsequently be absorbed by the solar cell and generate an electron-hole pair. Spectral conversion with DC is most beneficial for solar cells with a smaller band-gap where thermalization losses are the major loss factor. This process is also called as: quantum cutting, quantum splitting and multi-photon emission (MPE) or photon cascade emission (PCE). The theoretical possibility of down-conversion phenomena was first proposed by Dexter in 1957 [2]. Lanthanides are well suited for their use in both DC and UC due to their wide energy level structure that allows for efficient spectral conversion [3]. Trupke et al. are the first who have practically tested the effect of using either up-conversion or down-conversion materials in combination with solar cells [4]. Under the assumptions of an ideal down-converter on the front side of a silicon solar cell under non-concentrated sunlight, they have shown using detailed-

*Corresponding author. Tel.: +82 42 860 3449.
E-mail address: sdhan@kier.re.kr (S.-D. Han).
[1]Permanent address: Centre for Materials for Electronics Technology (C-MET), IDA Phase-III, Cherlapally, HCL (Post), Hyderabad-500051, India.

0272-8842/$ - see front matter © 2012 Elsevier Ltd and Techna Group S.r.l. All rights reserved.
http://dx.doi.org/10.1016/j.ceramint.2012.08.002

balance calculations where the efficiency limit may increase to 36.6% [4]. Spectrum modification feature can be used to tune the emission spectra for specific applications. Thus, it is an important for the systematic research on the phosphors of rare earth ions doped different kinds of host materials having good thermal, electrical and optical properties [5].

YVO_4 is one of the most extensively used optical material because it has many outstanding features includes, excellent thermal, mechanical and optical properties. The experimental band gap of YVO_4 is 3.8 eV, whereas replacement of Y^{3+} sites with Bi^{3+} ions could result in a significant reduction in band gap, i.e., ~3.6 eV. Yttrium orthovanadate is a well-known host lattice which exhibits high luminescence efficiency [6,7]. The Bi^{3+} ion was proved to be an excellent sensitizer for several Ln^{3+} ions in YVO_4 host lattice with not only enhancing the emission intensity, but also improved the broadness of the excitation spectrum [8]. Depending upon the host matrix, Bi^{3+} ions may emit in the UV, green or red regions. Red luminescence was reported in $Bi_4Ge_3O_{12}$ at low temperature [9], while in other materials such as $GdBO_3$:Bi^{3+} and La_2SO_6:Bi^{3+}, UV-emission was observed [10]. The trivalent ytterbium was characterized by a very simple energy level scheme among the rare earth active ions, consists only two levels: $^2F_{7/2}$ a ground state and $^2F_{5/2}$ an excited state. The Yb^{3+} ions, as an activator and acceptor is ideally suitable for its use in the down-conversion of **c**-Silicon solar cells, based on its luminescence efficiency as close to 100% and also owing to its broad emission band from 900 to 1100 nm, which matches well with the band gap of **c**-Si (where the band gap, E_g=1.12 eV, ~1100 nm)[11]. However, the NIR-DC phenomena reported in literature are all originated from the transitions of rare earth ions, the combination of transition metal and rare earths for NIR-DC luminescence for **c**-Si solar cell application has not been studied, extensively [12].

Herein, we have studied the effect of pH value on particle size, morphology and luminescence properties of YVO_4:Bi^{3+} powder phosphors, where the phosphors have been synthesized by a novel co-precipitation technique. With the optimized Bi^{3+} ions as a sensitizer, YVO_4: Bi^{3+}, Yb^{3+} powder phosphors have been synthesized. The broad UV-excitation energy transfer from Bi^{3+} to Yb^{3+} ions in the NIR region was studied, which is very close to the band gap of **c**-Si solar cells. As per the spectral matching and down conversion phenomena, these phosphors as a thin DC layers on c-Si solar cells may contribute in a greater way in terms of power conversion efficiency.

2. Experimental

2.1. Synthesis of $Y_{1-x}VO_4$: Bi_x^{3+} ($0.005 \le x \le 0.05$ mol.) and $Y_{0.97-x}VO_4$: $Bi_{0.03}^{3+}$, Yb_x^{3+} ($0.01 \le x \le 0.2$ mol.) powder phosphors

For the synthesis of the proposed Yb, Bi co-doped vanadate phosphors, a co-precipitation technique followed by calcination was adopted, where the starting precursors were supposed to react at micro level and leads to homogeneous fine product. As we know that the different synthesis techniques may have some important effects on material microstructure, physical, optical and luminescence properties [13].

Yttrium oxide (Y_2O_3) (99.99%, Aldrich make), ammonium metavanadate (NH_4VO_3) (99+%), bismuth oxide (Bi_2O_3)-(99.99%), ytterbium oxide (Yb_2O_3)(99.99%), ethylene glycol (99.99%), nitric acid (98%) and ammonia (NH_3) solution (assay 28–30%,) of Aldrich make were used as the starting precursors. Initially, Y_2O_3, Yb_2O_3, Bi_2O_3 and NH_4VO_3 were dissolved in concentrated nitric acid with stirring and moderate heating on hot plate. After complete dissolution a certain volume of ethylene glycol was added to the resultant solution as a surfactant. The pH of the resultant solution was maintained from 7 to 10 with drop wise addition of NH_4OH, under vigorous stirring. A slightly yellow colour precipitate was formed, which was further allowed to stir for minimum 1 h. The obtained precipitate was washed thoroughly with D.I water and ethanol, in order to remove the unreacted remnants. The obtained mass was dried in an electric oven at 120 °C. The dried powders were crushed in an agate mortar and pre-heated from room temperature to 700 °C for 2 h. Simultaneously, the temperature was increased to 1100 °C and sintered the powders for 5 h, in order to get better crystalinity and an intense luminescence. The effect of pH on particle size and morphology was studied only for YVO_4:Bi_x^{3+} phosphors. SEM measurements revealed that the phosphors synthesized with pH-9.0 have shown the fine particle size with regular shape and loosely bound among the other pH conditions. Hence, the remaining $Y_{0.97-x}VO_4$:$Bi_{0.03}^{3+}$, Yb_x^{3+} phosphors, have been synthesized with the optimized pH-9.0 condition.

2.2. Characterization

The crystalinity and phase purity of the synthesized powder phosphors have been investigated by X-ray Diffraction (XRD), using Rigaku X-ray Diffractometer D/max 2500 ultima having Cu K_α radiation (λ=1.5406 Å), at 40 kV tube voltage and 40 mA tube current. XRD patterns were measured with the diffraction angle (2Θ) ranging, $10^\circ \le 2\Theta \le 70^\circ$. Photoluminescence (PL) spectra of the produced phosphors were measured using Minolta Spectoradiometer, CS-1000. Before, measuring PL ~5 g of phosphor each sample was spread onto a flat surface of 50 mm dia and 1 mm thickness. A 365 nm UV-lamp mounted on top of the sample with a certain height was used as an excitation source. The PL measurements were carried out at room temperature with in the wavelength region 400–700 nm. The chromaticity coordinates (x, y) as per Commission International de L'Eclairage (CIE) were measured using the same set-up of Minolta spectroradiometer. The surface morphology and crystallite sizes of the synthesized phosphors were studied using Hitachi, S-4700 scanning electron microscope (SEM) with Horiba energy dispersive X-ray analysis (EDAX) attachment. The measurement conditions like accelerating voltage (kV), working

distance (mm), magnification (× K) and scale bar employed for each sample were available on micrographs. The chemical bonding/functional group details of the prepared phosphors were measured using Shimadzu 8900, Fourier transform-infrared (FT-IR) spectrometer with potassium bromide (KBr) pellet technique. The FT-IR spectral measurements were carried out in the wavenumber region 400–4000 cm^{-1}.

3. Results and discussion

Fig.1 shows the XRD patterns of $Y_{0.97}VO_4$: $Bi^{3+}_{0.03}$ powder phosphors, prepared through a co-precipitation technique, followed by heat-treatment at 1100 °C for 5 h. The above composition phosphor was synthesized with various pH values: pH-6.0, 7.0, 9.0 and 10.0, where the heat-treatment process was maintained as the same. The obtained XRD profiles were well matched with the JCPDS file No: 72-0861 of YVO_4. The produced phosphors possesses tetragonal phase with body centered, where the cell parameters are: $a=7.123$ and $c=6.292$. From the XRD profiles, it is noted that the pH values while precipitation have not altered the crystal structure, indicated by without any appreciable peak shifts in the diffraction profiles. Even after the substitution of Y^{3+} sites with Bi^{3+}, there was no any notable change in the crystal structure of YVO_4.

Fig. 2(a–e) shows the XRD profiles of (a) $Y_{0.96}VO_4$: $Yb^{3+}_{0.01}$, $Bi^{3+}_{0.03}$, (b) $Y_{0.94}VO_4$: $Yb^{3+}_{0.03}$, $Bi^{3+}_{0.03}$, (c) $Y_{0.92}VO_4$: $Yb^{3+}_{0.05}$, $Bi^{3+}_{0.03}$, (d) $Y_{0.87}VO_4$: $Yb^{3+}_{0.1}$, $Bi^{3+}_{0.03}$ and (e) $Y_{0.77}VO_4$: $Yb^{3+}_{0.2}$, $Bi^{3+}_{0.03}$, powder phosphors. Bi^{3+} co-doped with various amounts of Yb^{3+}, X-ray profiles were also found to be in line with tetragonal phase of YVO_4 (JCPDS file no: 72-0861). No additional diffraction peaks that could be attributed to impurity phases were observed; indicating that an appreciable amount of Bi^{3+} and Yb^{3+} co-doping to YVO_4 host matrix does not have altered the host crystal structure. The doped Yb^{3+} and Bi^{3+} ions might have occupied the Y^{3+} sites, owing to their similar ionic radii (Y^{3+}, $r=0.09$ nm; Yb^{3+}, $r=0.087$ nm and Bi^{3+}, $r=0.103$ nm). The measured diffraction patterns were in good agreement with the reported literature [14,15]. From the XRD measurements, it is concluded that the produced powder phosphors were phase pure and possesses tetragonal phase.

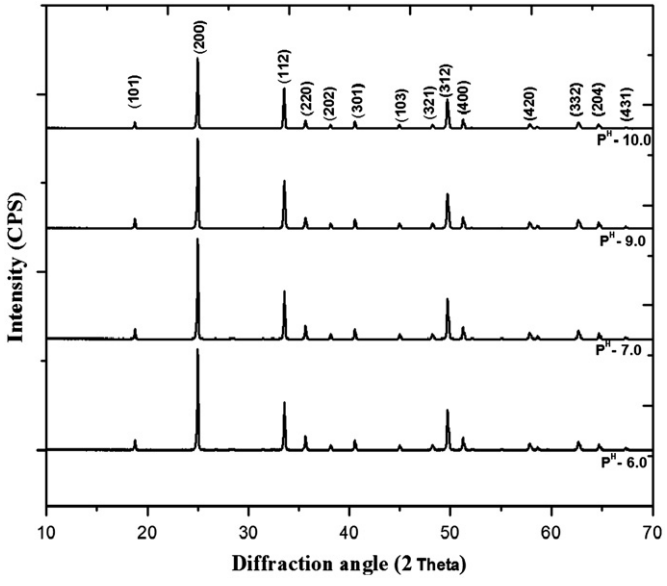

Fig. 1. XRD patterns of $Y_{0.97}VO_4$: $Bi^{3+}_{0.03}$ powder phosphors, synthesized with various pH values: 6.0, 7.0, 9.0 and 10.0.

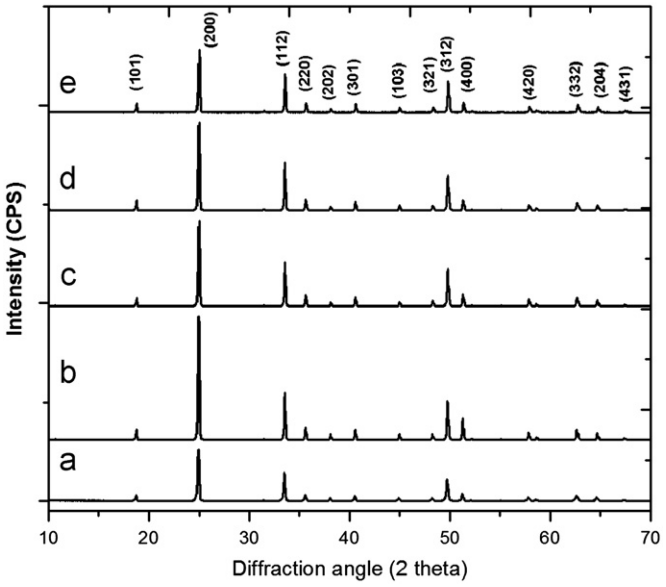

Fig. 2. XRD profiles of (a) $Y_{0.96}VO_4$: $Yb^{3+}_{0.01}$, $Bi^{3+}_{0.03}$, (b) $Y_{0.94}VO_4$: $Yb^{3+}_{0.03}$, $Bi^{3+}_{0.03}$, (c) $Y_{0.92}VO_4$: $Yb^{3+}_{0.05}$, $Bi^{3+}_{0.03}$ (d) $Y_{0.87}VO_4$: $Yb^{3+}_{0.1}$, $Bi^{3+}_{0.03}$ and (e) $Y_{0.77}VO_4$: $Yb^{3+}_{0.2}$, $Bi^{3+}_{0.03}$, powder phosphors.

Crystallinity, particle size and surface morphology of the phosphors, could show appreciable influence on photo-luminescence properties. In recent years more attention has been paid to the synthesis of inorganic phosphors with fine particle size, controlled morphologies and high luminescence efficiencies [16]. Compared to the conventional solid state reaction methods, wet chemical routes have been proved to be more powerful techniques for preparing phase pure and well crystalline phosphors, such as co-precipitation technique, where the multiple intermediate grinding and calcinations were not required. The controlled precipitation will take care the above two steps. Fig. 3(a–d) shows the SEM images of YVO_4: $Bi^{3+}_{0.03}$ prepared with distinct pH values (a) pH-6.0; (b) pH-7.0; (c) pH-9.0 and (d) pH-10.0. It is well known that the pH value of the reaction solutions maintained while co-precipitation will affect the nucleation and growth of particles, which consequently can modify the particle morphology and crystallite size of the final product. Fig. 3(a) shows the stone like layered structure of YVO_4: $Bi^{3+}_{0.03}$ with the particle size in the range, 3–6 μm. The small particles dispersed on larger particles might be the crushed particles during hand milling of the lumps, after sintering. However, the big particles were noted to be loosely bound. In the case of samples prepared with pH-7.0 (Fig. 3(b)), pH-9.0 (Fig. 3(c)) and pH-10 (Fig. 3(d)), no significant changes in the morphology were observed except variation

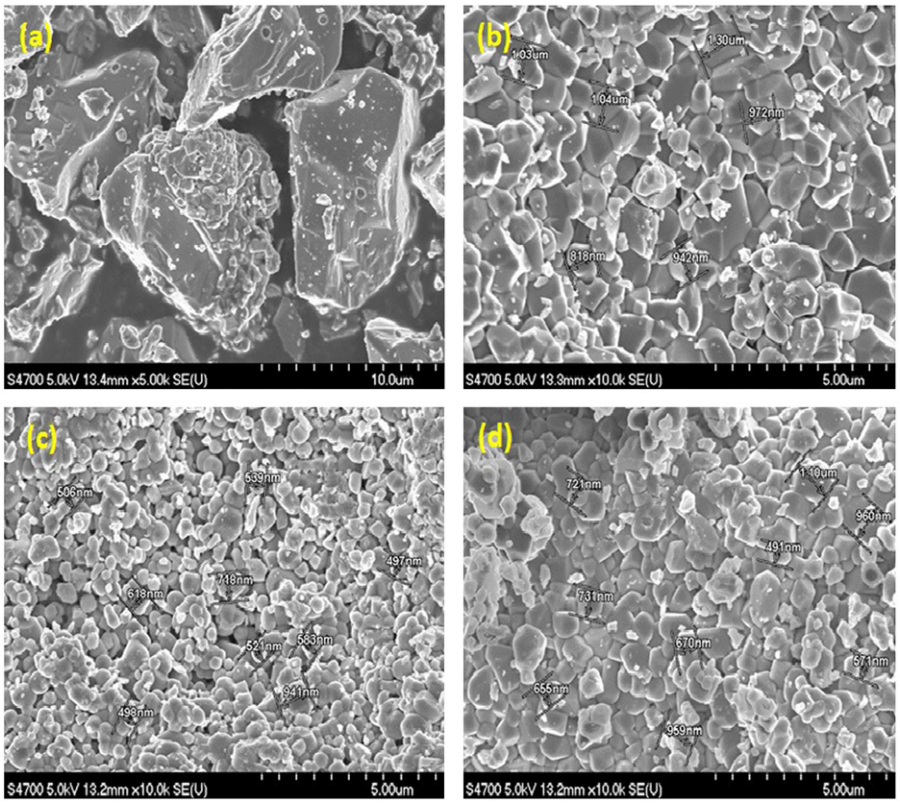

Fig. 3. SEM images of $Y_{0.97}VO_4$: $Bi^{3+}_{0.03}$ powder phosphors produced with various pH values: (a) pH −6.0, (b) pH −7.0, (c) pH −9.0 and (d) pH −10.0.

in the particle size. Phosphor with pH-9.0 has shown fine particle size in the range 500–600 nm, with regular shape and free of agglomerations. The phosphor produced with pH-10 has also grown regular shaped crystallites with size in the range 500–900 nm. The phosphors obtained with pH more than 7.0, possesses flat surface with loosely bound, which were good for making thin films by using screen printing or polymer embedded coatings. Zhang et.al have also been experienced the changes in the morphology of $LaVO_4$ phosphors synthesized with acidic conditions in hydrothermal synthesis. According to their report, it is understood that the stability of lanthanide vanadates were lower in acidic conditions as per their chemical properties, which leads to the formation of irregular microstructures. This is mainly due to the balance of crystallization and dissolution of lanthanide vanadates under acidic conditions. The lattice constants of lanthanide vanadates were also slightly more in acidic media [17].

Fig. 4 shows the SEM micrographs of (a1) $Y_{0.96}VO_4$: $Yb^{3+}_{0.01}$, $Bi^{3+}_{0.03}$ and (b1) $Y_{0.87}VO_4$: $Yb^{3+}_{0.1}$, $Bi^{3+}_{0.03}$, powder phosphors, synthesized with pH-9.0. It is obvious from the SEM images that with the incorporation of Yb into YVO_4:Bi^{3+} phosphors, the morphology and particle sizes have found to be moderately changed. The maximum crystallite size observed for these phosphors are at around 1.5 μm.

Fig. 4 shows the energy dispersive X-ray analysis (EDAX) spectra of (a2) $Y_{0.96}VO_4$: $Yb^{3+}_{0.01}$, $Bi^{3+}_{0.03}$ and (b2) $Y_{0.87}VO_4$: $Yb^{3+}_{0.1}$, $Bi^{3+}_{0.03}$, powder phosphors. The EDAX spectra elucidate the qualitative analysis of the elements Y, V, O, Bi and Yb. EDAX technique is not an accurate tool for the elemental quantification compared with the standard acid dissolution techniques, such as ICP-OES, ICP-MS and AAS. However, the obtained dopant (Yb^{3+}, Bi^{3+}) concentrations are well matched with the precursor concentrations with ± 0.004%, error. One can see clearly, that as the Yb^{3+}-concentration increases from 0.01 to 0.1 mol., the intensity of Yb-EDAX speak has also been increased, accordingly. As per the Beers–Lambert law, the peak intensity is directly proportional to the concentration of the element. The pink border area on the SEM images indicates, the area chosen for EDAX measurements.

Fig. 5(a–d) shows, the FT-IR spectra of (a) $Y_{0.96}VO_4$: $Yb^{3+}_{0.01}$, $Bi^{3+}_{0.03}$, (b) $Y_{0.87}VO_4$: $Yb^{3+}_{0.1}$, $Bi^{3+}_{0.03}$, (c) $Y_{0.77}VO_4$: $Yb^{3+}_{0.2}$, $Bi^{3+}_{0.03}$ and (d) $Y_{0.97}VO_4$: $Bi^{3+}_{0.03}$ powder phosphors, measured in the frequency region 400–4000 cm^{-1}. Modes, in the region observed are due to the vanadium–oxygen (V–O) stretching vibrations of $[VO_4]^{3-}$ group and the other metal–oxygen (M–O) (M = Y, Bi and Yb) bonds present in the phosphors. The weak, but intense signal of Y–O bond was found to be at around 449.5 cm^{-1}. It is obvious from the FT-IR spectra that for singly doped Bi^{3+} and with Yb^{3+} co-doped YVO_4, there was no any notable spectral shift in the peak position of M–O bond. But the intensity of M–O peak, noted to be increased with Yb-content from 0.01 to 0.2 mol. An intense and broad

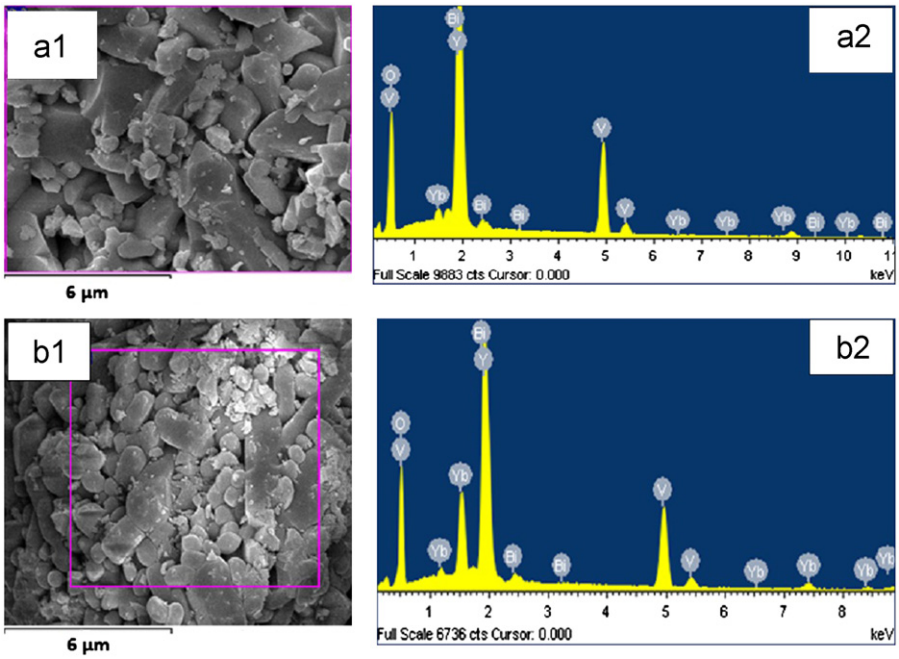

Fig. 4. SEM/EDAX micrographs of (a1, a2) $Y_{0.96}VO_4$: $Yb^{3+}_{0.01}$, $Bi^{3+}_{0.03}$ and (b1, b2) $Y_{0.87}VO_4$: $Yb^{3+}_{0.1}$, $Bi^{3+}_{0.03}$ powder phosphors, respectively. (For interpretation of the references to color in this figure legend, the reader is referred to the web version of this article.)

absorption peak in the wavenumber region 500–1000 cm^{-1} with its centre at 837 cm^{-1} was attributed to V–O stretching mode. This peak is noted to be broadening for Yb, co-doped phosphors compared to Bi^{3+}, singly doped vanadates. The peaks attributed to O–H stretching vibration and H–O–H bending vibrational modes due to absorption of moisture on the surface of the phosphor powders, as reported by the other researchers [18–21], has not been observed in the case of our samples. From the FT-IR spectral measurements, it is understood that the phosphors produced at our laboratory are more stable to moisture and other gas (CO_2) contaminations from the environment. It is concluded, that the observed V–O stretching modes of FT-IR measurements have supported the vanadate phase purity of the produced phosphors, as per XRD results.

Fig. 6(i) shows the photoluminescence excitation (PLE) spectra of the phosphor $Y_{0.97}VO_4$: $Bi^{3+}_{0.03}$ prepared with different pH values 6.0, 7.0, 9.0 and 10, monitored at emission wavelength, $\lambda_{em}=550$ nm. There is an intense and broad excitation band with its maximum at around 340 nm in the wavelength region 280–370 nm. It is confirmed that the strong broad excitation band comes from the absorption of Bi^{3+}, ions. Bi^{3+} ions, have an outer $6S^2$ electronic configuration with ground state of $^1S_0$, the excited states have 6s6p configuration and are split into the $^3P_0$, $^3P_1$, $^3P_2$ and $^1S_1$ levels in sequence of increasing energy. Transitions between $^1S_0$ and $^3P_0$, $^3P_1$ or $^3P_2$ are spin forbidden. However, the $^3P_1$ level undergoes mixing with $^1P_1$ by spin–orbit coupling, allowing the $^1S_0 \rightarrow {}^3P_1$ transitions that are frequently observed in PL measurements. As per the literature, we consider that the strong broad excitation band at 340 nm is ascribed to

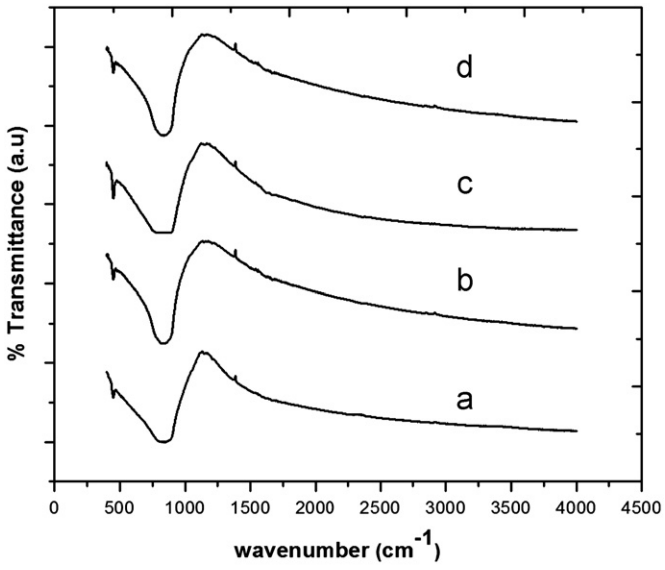

Fig. 5. FT-IR spectra of (a) $Y_{0.96}VO_4$: $Yb^{3+}_{0.01}$, $Bi^{3+}_{0.03}$, (b) $Y_{0.87}VO_4$: $Yb^{3+}_{0.1}$, $Bi^{3+}_{0.03}$, (c) $Y_{0.77}VO_4$: $Yb^{3+}_{0.2}$, $Bi^{3+}_{0.03}$ and (d) $Y_{0.97}VO_4$: $Bi^{3+}_{0.03}$, powder phosphors.

$^1S_0 \rightarrow {}^3P_1$, transition of Bi^{3+}, ions [22–27]. From the excitation spectra, it can be seen that the intensity of the excitation band $^1S_0 \rightarrow {}^3P_1$ is found to be varied with the pH value. The phosphor $Y_{0.97}VO_4$: $Bi^{3+}_{0.03}$ with pH-9.0 has shown more intense broad band owing to the small and regular particle size, observed from the SEM micrographs [Fig. 3(c)].

Fig. 6(ii) shows the photoluminescence (PL) spectra of the phosphors $Y_{0.97}VO_4$: $Bi^{3+}_{0.03}$ synthesized with different pH values, i.e., at pH=6.0, 7.0, 9.0 and 10. Upon, 340 nm

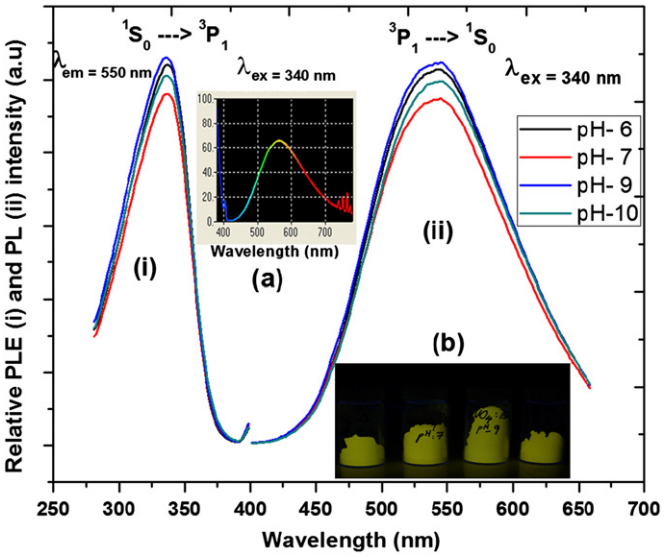

Fig. 6. Photoluminescence excitation (PLE) (i) and photoluminescence (PL) (ii) spectra of the phosphor, $Y_{0.97}VO_4$: $Bi^{3+}_{0.03}$ prepared with different pH values 6.0, 7.0, 9.0 and 10.0, respectively. (a) PL spectrum of the phosphors $Y_{0.97}VO_4$: $Bi^{3+}_{0.03}$ (with pH-9.0), which was recorded with spectroradiometer with the aid of 365 nm, UV-lamp as an excitation source. (b) Photograph shows, greenish yellow emission, upon 365 nm UV-excitation of the phosphors, $Y_{0.97}VO_4$: $Bi^{3+}_{0.03}$ prepared with different pH values: 6.0, 7.0, 9.0 and 10.0 (from left to right). (For interpretation of the references to color in this figure legend, the reader is referred to the web version of this article.)

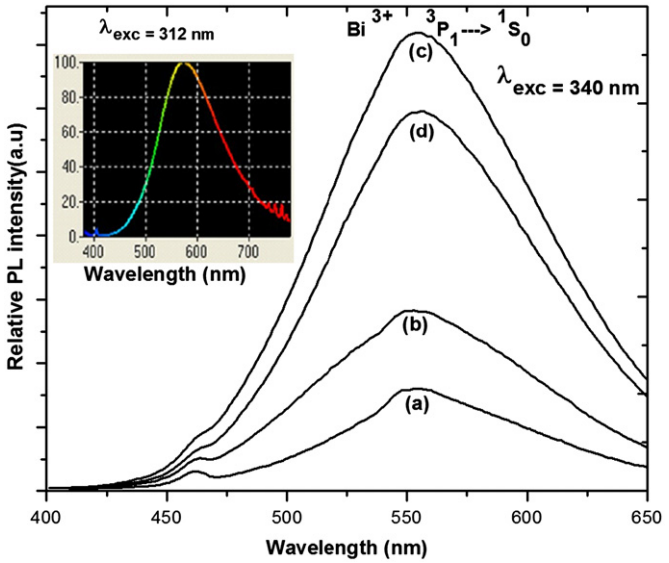

Fig. 7. Photoluminescence (PL) spectra of (a) $Y_{0.995}VO_4$: $Bi^{3+}_{0.005}$, (b) $Y_{0.99}VO_4$: $Bi^{3+}_{0.01}$, (c) $Y_{0.97}VO_4$: $Bi^{3+}_{0.03}$ and (d) $Y_{0.95}VO_4$: $Bi^{3+}_{0.05}$ powder phosphors, monitored at λ_{exc}=340 nm. The inset shows, PL spectrum of the phosphors $Y_{0.97}VO_4$: $Bi^{3+}_{0.03}$ (with pH-9.0), which was recorded with spectroradiometer with the aid of 312 nm, UV-lamp as an excitation source.

excitation these phosphors have exhibited a broad emission band centered at 557 nm, corresponding to the transition of Bi^{3+}: $^3P_1 \rightarrow {}^1S_0$, which is also ascribed as due to $V^{5+} \rightarrow Bi^{3+}$ charge transfer luminescence [26,27]. From the emission spectra it is noted that the intensity of the emission peak $^3P_1 \rightarrow {}^1S_0$, observed to be varied with the pH value of phosphor, at which it has been synthesized. The phosphor prepared with pH-9.0 has shown more intense broad emission band among the other phosphors, where it consists of regular shape and fine particle size [Fig. 3(c)].

Fig. 6(a) shows the PL spectrum of the phosphors $Y_{0.97}VO_4$: $Bi^{3+}_{0.03}$, produced with pH-9.0. The emission spectrum has been recorded with spectroradiometer, with the aid of 365 nm UV lamp, by spreading the sample as a thick film, as explained in the experimental part. An intense broad band emission observed from 400 to 700 nm with its centre at 571 nm is attributed to Bi^{3+}: $^3P_1 \rightarrow {}^1S_0$, which indicates an intense greenish–yellow emission. This is confirmed by the photograph shown at Fig. 6(b), upon 365 nm UV-irradiation. In Fig. 6(a), a group of small peaks observed above 700 nm are due to noise level, we normally observed for all the samples.

With the investigation of the effect of pH value on particle size and emission intensities, a series of phosphors have been synthesized in order to optimize the dopant Bi^{3+} concentration, with YVO_4 host matrix. Fig. 7 shows the emission spectra of (a) $Y_{0.995}VO_4$: $Bi^{3+}_{0.005}$, (b) $Y_{0.99}VO_4$: $Bi^{3+}_{0.01}$, (c) $Y_{0.97}VO_4$: $Bi^{3+}_{0.03}$ and (d) $Y_{0.95}VO_4$: $Bi^{3+}_{0.05}$ powder phosphors, monitored excitation wavelength, at λ_{exc}=340 nm. It is obvious from the emission spectra that the broad band emission (Bi^{3+}: $^3P_1 \rightarrow {}^1S_0$, transition) intensity is noted to be increased with the activator Bi^{3+} concentration from 0.005 to the value of 0.03 mol., beyond that the intensity is found to be decreased, owing to the well-known concentration quenching effect of Bi^{3+} ions. Thus, the optimum dopant, Bi^{3+} ions concentration was measured to be 3 mol. %. A small blue peak at 460 nm observed from the emission spectra is originated from the energy transition of molecular or orbital of $[VO_4]^{3-}$ group, which is in good agreement with the literature reports [8,28,29].

From the emission spectra (Fig. 7(a–d)), it can be seen clearly that with λ_{exc}=340 nm there was no any remarkable peak shift in the broad band emission with variable Bi^{3+} concentration. The inset of Fig. 7 shows the PL spectrum of the optimized phosphor composition $Y_{0.97}VO_4$:$Bi^{3+}_{0.03}$ measured using Minolta spectroradiometer, upon 312 nm UV-lamp excitation. As explained in the previous session a group of small peaks beyond 700 nm are owing to the noise level.

The development of crystalline silicon solar cells could greatly benefit from down-conversion (DC) phosphors, with their emissions located just above the band gap of **c**-Si (~1100 nm). If conversion of one irradiated UV–visible (300–500 nm) photon into two NIR (~ 1100 nm) photons is realized, the energy loss due to the thermalization in **c**-Si solar cells could be minimized [8,30]. Rare earth ions with abundant energy levels are good candidates for DC-process. The trivalent ytterbium is characterized by a very simple energy level scheme among the rare earth active ions, consisting in only two energy levels: $^2F_{7/2}$ a ground state and $^2F_{5/2}$, an excited state. However, it is important to find a

suitable sensitizer that can efficiently down convert the broad band 300–575 nm light into ~1000–1100 nm NIR emission of Yb^{3+}, via energy transfer. It is well-known that co-dopants can modify crystal structure, morphology and PL properties of phosphors. A few dopants, even a little an amount are propitious to high luminescence efficiency [22]. Since, Bi^{3+} ions with $6S^2$ electronic configuration can serve as both an activator and a sensitizer for luminescence materials, we would like to study the effect of Bi^{3+} ions on NIR emission of Yb^{3+}, dopant in YVO_4 host lattice. In this connection, a series of phosphors by fixing an optimized amount of Bi^{3+} as 3 mol. % and by varying the concentration of Yb^{3+} from 0.01 to 0.2 mol. have also been synthesized by co-precipitation technique, as follows:

Fig. 8 shows the photoluminescence excitation (PLE) (i) and photoluminescence (PL)(ii) spectra of (a) $Y_{0.96}VO_4$: $Yb^{3+}_{0.01}$, $Bi^{3+}_{0.03}$, (b) $Y_{0.94}VO_4$: $Yb^{3+}_{0.03}$, $Bi^{3+}_{0.03}$, (c) $Y_{0.92}VO_4$: $Yb^{3+}_{0.05}$, $Bi^{3+}_{0.03}$, (d) $Y_{0.87}VO_4$: $Yb^{3+}_{0.1}$, $Bi^{3+}_{0.03}$ and (e) $Y_{0.77}VO_4$: $Yb^{3+}_{0.2}$, $Bi^{3+}_{0.03}$ powder phosphors, respectively. The excitation spectra have shown a broad excitation band owing to Bi^{3+}: $^1S_0 \rightarrow {}^3P_1$, transition where its intensity is measured to be gradually reduced with increased Yb^{3+}-content. An appreciable peak shift was not observed, however, the FWHM of the broad band is noted to be varied with Yb-content.

From the emission spectra (Fig. 8(ii)), it is revealed that the intensity of the broad band emission of Bi^{3+}: $^3P_1 \rightarrow {}^1S_0$ is noted to be reduced gradually with Yb content from 0.01 to 0.2 mol., due to the concentration quenching of Yb^{3+}, ions. As discussed earlier the weak blue peak observed at 460 nm is due to the energy transition of molecular or orbital of $[VO_4]^{3-}$ group, from the host matrix. However, the phosphor with chemical composition, $Y_{0.96}VO_4$: $Yb^{3+}_{0.01}$, $Bi^{3+}_{0.03}$ have shown an intense greenish–yellow emission among the synthesized. The inset photograph Fig. 8(ii), shows the diminishing trend of greenish yellow emission from left to right (a→e), with increased concentration of Yb^{3+}-ions.

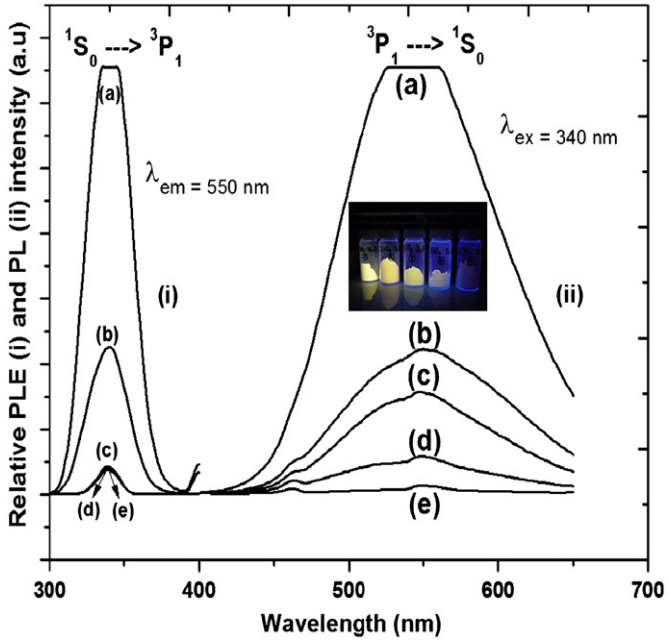

Fig. 8. Photoluminescence excitation (PLE) (i) and photoluminescence (PL) (ii) spectra of (a) $Y_{0.96}VO_4$: $Yb^{3+}_{0.01}$, $Bi^{3+}_{0.03}$, (b) $Y_{0.94}VO_4$: $Yb^{3+}_{0.03}$, $Bi^{3+}_{0.03}$, (c) $Y_{0.92}VO_4$: $Yb^{3+}_{0.05}$, $Bi^{3+}_{0.03}$, (d) $Y_{0.87}VO_4$: $Yb^{3+}_{0.1}$, $Bi^{3+}_{0.03}$ and (e) $Y_{0.77}VO_4$: $Yb^{3+}_{0.2}$, $Bi^{3+}_{0.03}$ powder phosphors, respectively. The inset of (ii) is the photograph displays, greenish yellow emission, upon 365 nm UV-excitation of the phosphors: (a)→(e) from left to right. (For interpretation of the references to color in this figure legend, the reader is referred to the web version of this article.)

Fig. 9 shows the near infrared (NIR) emission spectra of: (a) $Y_{0.96}VO_4$: $Yb^{3+}_{0.01}$, $Bi^{3+}_{0.03}$, (b) $Y_{0.94}VO_4$: $Yb^{3+}_{0.03}$, $Bi^{3+}_{0.03}$, (c) $Y_{0.92}VO_4$: $Yb^{3+}_{0.05}$, $Bi^{3+}_{0.03}$, (d) $Y_{0.87}VO_4$: $Yb^{3+}_{0.1}$, $Bi^{3+}_{0.03}$ and (e) $Y_{0.77}VO_4$: $Yb^{3+}_{0.2}$, $Bi^{3+}_{0.03}$ powder phosphors, measured with Bi^{3+}: $^1S_0 \rightarrow {}^3P_1$, UV-excitation wavelength, i.e., at λ_{exc}=340 nm. From the NIR emission spectra, a broad emission peak owing to Yb^{3+}: $^2F_{5/2} \rightarrow {}^2F_{7/2}$ is observed from 1020 to 1060 nm having its center at 1039 nm. The intensity of Yb^{3+}: $^2F_{5/2} \rightarrow {}^2F_{7/2}$ peak is found to be decreased with Yb-content from 0.01 to 0.05 mol., and then it is observed to be increased remarkably with Yb-0.1 mol., beyond that noted to be quenched. Thus, the phosphor with composition $Y_{0.87}VO_4$: $Yb^{3+}_{0.1}$, $Bi^{3+}_{0.03}$ have shown an intense NIR emission among the produced phosphors, due to the efficient energy transfer from Bi^{3+} to Yb^{3+} ions.

Recently, Ferhi et al. have reported the NIR emission of Yb^{3+}-doped $LaPO_4$ phosphors with 925 nm excitation, where they have been observed a broad band NIR emission from 940 to 1100 nm, with distinct NIR emission peaks attributed to the transitions from the sub-levels of

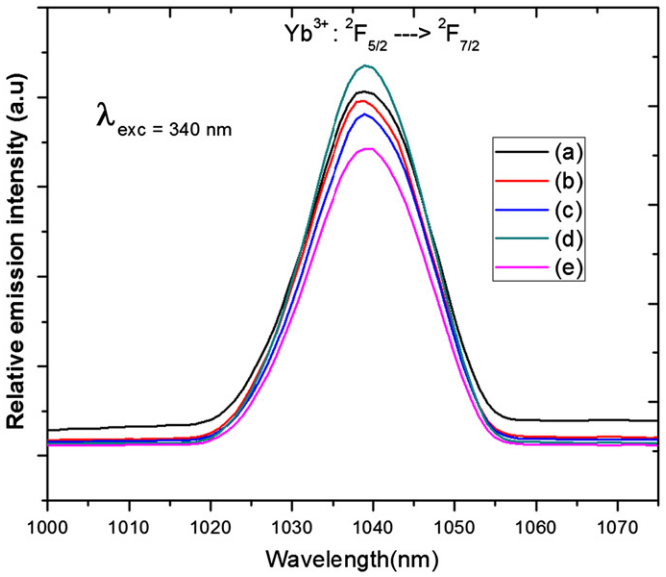

Fig. 9. Near infrared (NIR) emission spectra of: (a) $Y_{0.96}VO_4$: $Yb^{3+}_{0.01}$, $Bi^{3+}_{0.03}$, (b) $Y_{0.94}VO_4$: $Yb^{3+}_{0.03}$, $Bi^{3+}_{0.03}$ (c) $Y_{0.92}VO_4$: $Yb^{3+}_{0.05}$, $Bi^{3+}_{0.03}$, (d) $Y_{0.87}VO_4$: $Yb^{3+}_{0.1}$, $Bi^{3+}_{0.03}$ and (e) $Y_{0.77}VO_4$: $Yb^{3+}_{0.2}$, $Bi^{3+}_{0.03}$ powder phosphors, measured with Bi^{3+}: $^1S_0 \rightarrow {}^3P_1$, UV-excitation, λ_{exc}=340 nm. (For interpretation of the references to color in this figure legend, the reader is referred to the web version of this article.)

$^2F_{5/2} \rightarrow {}^2F_{7/2}$. The observed peaks are assigned to the four stark levels of the ground $^2F_{7/2}$ state based on the emission spectra of Yb^{3+} in phosphate hosts with reference to Guzik et al. [31]. They observed four NIR emission peaks with centres at 976, 989, 1016 and 1030 nm [32]. Unlike the other reports [8], where they have been observed the Bi^{3+}/Yb^{3+}, NIR emission at 983 nm with Bi^{3+}, UV- 340 nm excitation, in the present work, the same broad band NIR emission of Yb^{3+}: $^2F_{5/2} \rightarrow {}^2F_{7/2}$ peak has been measured at 1039 nm. The shift in the NIR emission peak could be possibly due to the fine particle size of the produced phosphors, by co-precipitation technique compared to the conventional solid state reactions. The NIR emission observed at 1039 nm is more close to the band gap of **c**-Si solar cells ($E_g = 1.12$ eV; ~1100 nm). By applying these phosphors as DC layers on **c**-Si solar cells, one can achieve a great response in power conversion measurements, owing to the spectral matching phenomena.

Fig. 10 shows the schematic energy level diagram of energy transfer from Bi^{3+} ions to Yb^{3+} via cooperative energy transfer, where the Bi^{3+}: $^3P_1$, excited state was situated about twice the energy level of the Yb^{3+}: $^2F_{5/2} \rightarrow {}^2F_{7/2}$, and Yb^{3+} has no other levels up to the UV-region. So, the cooperative energy transfer of Bi^{3+}: $^3P_1 \rightarrow Yb^{3+}$: $^2F_{5/2} \rightarrow {}^2F_{7/2}$ can therefore be a dominant relaxation route to achieve the Yb^{3+}: NIR emission. Upon 340 nm excitation, Bi^{3+} emission obtained in the wavelength region 400–700 nm, having its centre at 550–575 nm is attributed to the transition, $^3P_1 \rightarrow {}^1S_0$. Moreover, two NIR photons correspond to the Yb^{3+}: $^2F_{5/2} \rightarrow {}^2F_{7/2}$ transition is obtained after the absorption of a single UV-photon [33,34].

Thus, Bi^{3+} a metal ion with broad band and spin allowed absorption in the UV–greenish–yellow (300–575 nm) region is investigated to be an excellent broad band sensitizer for Yb^{3+}, NIR emission in the region ~1000–1100 nm via co-operative energy transfer from Bi^{3+} to Yb^{3+}, ions. In order to find out the practical application of these phosphors, in terms of power conversion efficiency, the produced phosphor powders were embedded in a transparent polymer films (with an optimized ratio) and applied them as a DC-layers on **c**-Si solar cells. These phosphors as DC-layers have shown a great response in power conversion efficiency, under AM 1.5G solar simulator. The chromaticity coordinates (x, y) of the produced phosphors were measured using Minolta Spectroradiometer. The measured color coordinates (x, y) for the better phosphor compositions: (1) $Y_{0.97}VO_4:Bi^{3+}_{0.03}$ (0.3996, 0.5214), (2) $Y_{0.96}VO_4:Yb^{3+}_{0.01}$, $Bi^{3+}_{0.03}$ (0.3617, 0.5132) and (3) $Y_{0.87}VO_4:Yb^{3+}_{0.1}$, $Bi^{3+}_{0.03}$ (0.3455, 0.4875) have been well fitted in the greenish–yellow region of the CIE chromaticity diagram, as shown in Fig. 11.

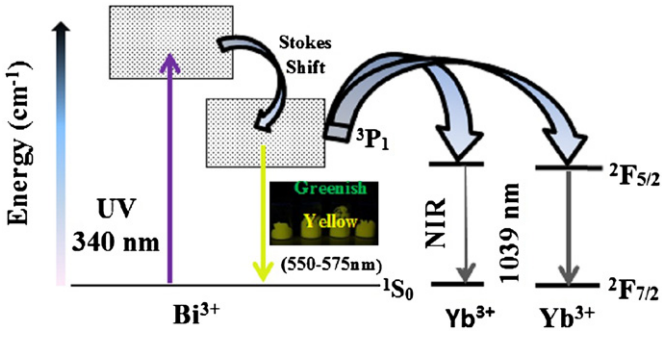

Fig. 10. Schematic energy level diagram of energy transfer from Bi^{3+} to Yb^{3+}, ions via the cooperative energy transfer. (For interpretation of the references to color in this figure legend, the reader is referred to the web version of this article.)

4. Conclusions

In summary, it is concluded that the highly efficient YVO_4: Bi^{3+} and YVO_4: Yb^{3+}, Bi^{3+}, powder phosphors have been successfully synthesized, through a novel co-precipitation technique. The effects of pH on crystallite size, morphology and luminescence properties have been investigated. The synthesized phosphors are having particle size in the range 400 to 1500 nm with regular shape and free of agglomerations. XRD profiles revealed that the powders produced are more crystalline, phase pure and possesses body centered tetragonal phase of YVO_4. FT-IR measurements elucidate, a weak but intense absorption peak of M–O (M = Y, Yb and Bi) bond at around 449 cm^{-1} and a broad absorption peak at 837 cm^{-1} owing to $[VO_4]^{3-}$, stretching mode. Unlike, the other reports (blue, green color) the produced phosphors have shown an intense greenish–yellow emission upon UV-excitation, owing to the fine particle size obtained via co-precipitation synthesis route. The optimum dopant concentration of Bi^{3+} ions, in YVO_4 host matrix was found to be 3 mol%. Both YVO_4: Bi^{3+} and YVO_4: Yb^{3+},

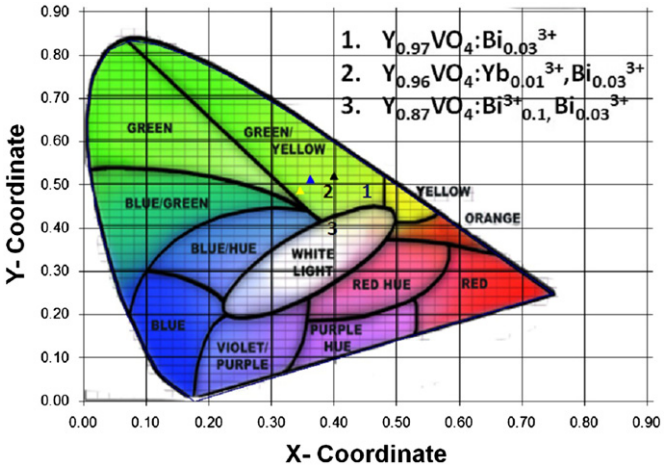

Fig. 11. CIE, chromaticity diagram indicating the colour coordinates of the phosphors: (1). $Y_{0.97}VO_4:Bi^{3+}_{0.03}$, (2) $Y_{0.96}VO_4$: $Yb^{3+}_{0.01}$, $Bi^{3+}_{0.03}$ and (3). $Y_{0.87}VO_4$: $Yb^{3+}_{0.1}$, $Bi^{3+}_{0.03}$, which have been fitted in the greenish–yellow region. (For interpretation of the references to color in this figure legend, the reader is referred to the web version of this article.)

Bi^{3+} have shown an intense broad band emission from 410 to 700 nm, owing to Bi^{3+}: $^3P_1 \rightarrow {}^1S_0$, transition. Upon, 340 nm UV-excitation with the spin allowed Bi^{3+}: $^1S_0 \rightarrow {}^3P_1$, the characteristic NIR emission of Yb^{3+} due to $^2F_{5/2} \rightarrow {}^2F_{7/2}$ transition was measured at 1039 nm, as a result of cooperative energy transfer from $Bi^{3+} \rightarrow Yb^{3+}$, ions. The observed NIR emission at 1039 nm is very close to the band gap of c-Si solar cells (i.e., $E_g = 1.12$ eV, ~1100 nm). Based on the systematic materials characterization and luminescence properties, the phosphors with composition; $Y_{0.96}VO_4$: $Bi^{3+}_{0.03}$, $Yb^{3+}_{0.01}$ and $Y_{0.87}VO_4$: $Bi^{3+}_{0.03}$, $Yb^{3+}_{0.1}$ are suggested to be the novel candidates for the down conversion of broad band, UV into visible/NIR emission with their transparent thin film form in front of crystalline-Silicon solar cells, for better harvesting the solar spectrum via spectral matching phenomena.

Acknowledgments

One of the authors, URB would like to thank Korean Federation of Science and Technology (KOFST), Korea for awarding Brain pool Fellowship and also express his gratitude to Dr. D. P. Amalnerkar, Executive Director and Dr. T. L. Prakash, Director of C-MET, India for allowing to carry out this research work at Korea Institute of Energy Research (KIER), Korea.

References

[1] R.A. Kerr, R.F. Service, What can replace cheap oil—and when?, Science 309 (5731) (2005) 101-101.
[2] D.L. Dexter, Possibility of luminescent quantum yields greater than unity, Physical Review 108 (3) (1957) 630–633.
[3] J.M. Maijer, L. Aarts, B.M.V. Ende, T.J.H. Vlugt, A. Maeijerink, Down conversion for solar cells in YF_3:Nd^{3+}, Yb^3, Physical Review B 81 (2010) 035107–035116.
[4] T. Trupke, A. Shalav, B.S. Richards, P. Wurfel, M.A. Green, Efficiency enhancement of solar cells by luminescent up-conversion of sun light, Solar Energy Materials and Solar Cells 90 (2006) 3327–3338.
[5] Y.J. Hsiao, T.H. Fang, L.W. Ji, Photoluminescence and preparation of $ZnNb_2O_6$ doped with Eu^{3+} and Tm^{3+} nanocrystals for solar cell, Materials Chemical and Physics 130 (2011) 1187–1190.
[6] A. Hulgnard, T. Gacoin, J.-P. Boilot, Synthesis and luminescence properties of colloidal YVO_4: Eu phosphors, Chemistry of Materials 12 (2000) 1090–1094.
[7] A.K. Levine, F.C. Papilla, A new, highly efficient red emitting cathodoluminescent phosphor (YVO_4: Eu) for color television, Applied Physics Letters 5 (1964) 118–120.
[8] X.Y. Huang, J.X. Wang, D.C. Yu, S. Ye, Q.Y. Zhang, X.W. Sun, Spectral conversion for solar cell efficiency enhancement using YVO_4: Bi^{3+}, Ln^{3+} (Ln=Dy, Er, Ho, Eu, Sm and Yb) phosphors, Journal of Applied Physics 109 (2011) 113526-1-113526-7.
[9] G. Blasse, C. Timmermans, The luminescence of some oxide bismuth and lead compounds, Journal of Solid State Chemistry 52 (1984) 222–232.
[10] V. Dotsenko, N. Efryushina, I. Berezovskaya, Luminescence properties of $GaBO_3$: Bi^3, Materials Letters 28 (1996) 517–520.
[11] J. Ueda, S. Tanabe, Visible to near infrared conversion in Ce^{3+}–Yb^{3+} co-doped YAG ceramics, Journal of Applied Physics 106 (2009) 043101–043106.
[12] Q.Y. Zhang, X.Y. Huang, Recent progress in quantum cutting phosphors, Progress in Materials Science 55 (2010) 353–427.
[13] L. Chen, G. Liu, Y. Liu, K. Huang, Synthesis and luminescence properties of YVO_4:Dy^{3+} nano-rods, Journal of Materials Processing and Technology 198 (2008) 129–133.
[14] Y. Lu, X. Chen, Plasmon-enhanced luminescence in Yb^{3+}:Y_2O_3 thin film and the potential for solar cell photon harvesting, Applied Physics Letters 94 (2009) 193110–193113.
[15] F. Real, B. Ordejon, V. Vallet, J. Flament, J. Schamps, Improvement of the ab initio embedded cluster method for luminescence properties of doped materials by taking into account impurity induced distortions: the example of Y_2O_3:Bi^3, Journal of Chemical Physics 131 (2009) 194501–194516.
[16] F. He, P. Yong, N. Niu, W. Wang, S. Gai, Dong Wang, J. Lin, Hydrothermal synthesis and luminescent properties of YVO_4:Ln^{3+} (Ln=Eu, Dy, and Sm) microspheres, Journal of Colloid and Interface Science 343 (2010) 71–78.
[17] S. Zhang, L. Wang, H. Peng, G. Li, K. Chen, Influence of P-doping on the morphologies and photoluminescence properties of $LaVO_4$:Tb^{3+} nanostructures, Materials Chemistry Physics 123 (2010) 714–718.
[18] C.T. Au, W.D Zhang, Oxidative dehydrogenation of propane over rare-earth ortho vanadates, Journal of Chemical Society, Faraday Transactions 93 (1997) 1195–1204.
[19] K. Byrappa, C.K. Chandrasekhar, B. Basvalingu, K.M. Loknatha Rai, S. Anandan, M. Yoshimura, Growth, morphology and mechanism of rare earth vanadate crystals under mild hydrothermal conditions, Journal of Crystal Growth 306 (2007) 94–101.
[20] B.V. Rao, G.B. Kumar, M. Jayasimhadri, K. Jang, H.S. Lee, S.S. Yi, J.H. Jeong, Photoluminescence and structural properties of $Ca_3Y(VO_4)_3$:RE^{3+} (=Sm^{3+}, Ho^{3+} and Tm^{3+}) powder phosphors for tri-colors, Journal of Crystal Growth 326 (2011) 120–123.
[21] G. Liu, X. Duan, H. Li, H. Dong, Hydrothermal synthesis, characterization and optical properties of novel fishbone-like $LaVO_4$: Eu^{3+} nanocrystals, Materials Chemistry and Physics 115 (2009) 165–171.
[22] G. Liu, Y. Zhang, J. Yin, W.F. Zhang, Enhanced photoluminescence of Sm^{3+}/Bi^{3+} co-doped Gd_2O_3 phosphors by combustion synthesis, Journal of Luminescence 128 (2008) 2008–2012.
[23] Y. Porter-Chapman, E.B. Courchesne, S.E. Derenzo, Bi^{3+} luminescence in $ABiO_2Cl$ (A=Sr, Ba) and $BaBiO_2Br$, Journal of Luminescence 128 (2008) 87–91.
[24] F. Kellendonk, T. Vander Belt, G. Blasse, On the luminescence of bismuth, cerium, and chromium and yttrium aluminum borate, Journal of Chemical Physics 76 (1982) 1194–1201.
[25] X.Y. Huang, X.H. Ji, Q.Y. Zhang, Broadband down conversion of ultraviolet light to near-infrared emission in Bi^{3+}–Yb^{3+}- co-doped Y_2O_3 phosphors, Journal of American Ceramic Society 94 (3) (2011) 833–837.
[26] A. Newport, J. Silver, A. Vecht, The synthesis of fine particle yttrium vanadate phosphors from spherical powder precursors using urea precipitation, Journal of Electrochemical Society 147 (2000) 3944–3947.
[27] S. Takeshita, T. Isobe, T. Sawayama, S. Niikura, Effects of the homogeneous Bi^{3+} doping process on photoluminescence properties of YVO_4:Bi^{3+}, Eu^{3+} nanophosphor, Journal of Luminescence 129 (2009) 1067–1072.
[28] L. Chen, K.J. Chen, C.C. Lin, C.I. Chu, S.F. Hu, M.H. Lee, R.S. Liu, Combinatorial approach to the development of a single mass YVO_4:Bi^{3+},Eu^{3+} phosphor with red and green dual colors for high color rendering white light-emitting diodes, Journal of Combinatorial Chemistry 12 (2010) 587–594.
[29] X. Wei, S. Huang, Y. Chen, C. Guo, M. Yin, W. Xu, Energy transfer mechanisms in Yb^{3+} doped YVO_4 near-infrared down conversion phosphor, Journal of Applied Physics 107 (2010) 103107–103111.
[30] T. Trupke, M.A. Green, P. Wurfel, Improving solar cell efficiencies by down-conversion of high-energy photons, Journal of Applied Physics 92 (2002) 1668–1674.

[31] M. Guzik, J. Levendzie Wicz, W. Szuszkiewicz, A. Walasek, Synthesis and optical properties of powders of lutetium and yttrium double phosphates-doped by ytterbium, Optical Materials 29, (2007) 1225-1230.

[32] M. Ferhi, K. Horchani, K. Horchani-Naifer, S. Hraiech, M. Ferid, Y. Guyot, G. Boulon, Near infrared and charge transfer luminescence of Yb^{3+}-doped $LaPO_4$ at room temperature, Radiation Measurements 46 (2011) 1033–1037.

[33] P. Vergeer, T.J.H. Vlugt, M.H.F. Kox, M.I. Den Hertog, J.P.J.M. Vander Earden, A. Maejerink, Quantum cutting by cooperative energy transfer in $Yb_xY_{1-x}PO_4$:Tb^3, Physical Review B 71 (2005) 014119–014129.

[34] X.Y. Huang, Q.Y. Zhang, Near-infrared quantum cutting via cooperative energy transfer in Gd_2O_3:Bi^{3+}, Yb^{3+} phosphors, Journal of Applied Physics 107 (2010) 063505–063508.